The methyl rotational potentials of $Ga(CH_3)_3$ derived by neutron spectroscopy

2002 J. Phys.: Condens. Matter 14 10145

(http://iopscience.iop.org/0953-8984/14/43/312)

INSTITUTE OF PHYSICS PUBLISHING JOURNAL OF PHYSICS: CONDENSED MATTER

J. Phys.: Condens. Matter **14** (2002) 10145–10157 PII: S0953-8984(02)37534-9

The methyl rotational potentials of $Ga(CH_3)_3$ derived by neutron spectroscopy

M Prager[1], J Combet[2], S F Parker[3], A Desmedt[4] and R E Lechner[4]

[1] Institut für Festkörperforschung, Forschungzzentrum Jülich, D-52425 Jülich, Germany
[2] Institut Laue Langevin, 156X, F-38042 Grenoble Cedex9, France
[3] ISIS Facility, Rutherford Appleton Laboratory, Chilton, Oxon OX11 0QX, UK
[4] Hahn-Meitner Institut, Glienickerstr. 100, D-14109 Berlin, Germany

Received 29 May 2002, in final form 29 August 2002
Published 18 October 2002
Online at stacks.iop.org/JPhysCM/14/10145

Abstract

High resolution neutron spectra of $Ga(CH_3)_3$ show tunnelling transitions between 4.5 and 19 μeV. The spectrum can be explained within the single-particle model on the basis of the monoclinic $C2/c$ ($Z = 16$) low temperature crystal structure of $Ga(CH_3)_3$ with six inequivalent methyl groups in the unit cell. The overlapping tunnelling lines prevent the extraction of temperature dependent linewidths which would allow us to assign the librational energies measured in the phonon density of states. Classical rotational motion is studied by quasielastic neutron scattering. Three activation energies could be extracted. Methyl librations, tunnelling energies and barrier heights are combined with consistent intensities into rotational potentials. Only the concerted application of all spectroscopic techniques yields a conclusive description.

(Some figures in this article are in colour only in the electronic version)

1. Introduction

Organometallic compounds represent one of the major classes of materials. Since these materials inherently contain methyl groups, rotational tunnelling spectroscopy is a suitable tool for their investigation. Some simple systems were studied in a systematic way. By varying the metal ion within the homologous series of group IV tetramethyl metal compounds from stable neopentane to the explosive tetramethyllead, a decreasing strength of the metal–carbon bond was observed [1]. The importance of intermolecular interactions—neglected in earlier studies—was clearly proven by spectra of matrix isolated molecules [2].

The group III trimethyl metal compounds form a similar and—due to their technical applications—possibly even more interesting class. The vicinity to the semiconducting elements in the periodic system and the instability of the materials make them an important starting material for doping Si or Ge with B, Al, Ga, In and Tl by thermal decomposition of the volatile molecules at the hot semiconductor surface. Aluminium alkyls are further used

as Ziegler–Natta catalysts for olefin polymerization. This application exploits the presence of unsaturated electron density. *Dimers* with weak electron deficient bonds are formed via bridging methyl groups. In the solid the crystal structure is $C2/c$ and again dimers $Al_2(CH_3)_6$ are the building units [3–6]. The aluminium atoms and the bridging carbons form a plane with an inversion centre at the centre of gravity of the dimer which yields three inequivalent types of methyl group [6]. With dimerization the number of bonds of the aluminium atom increases from three to four. Since the bridging methyl groups share the electron density of about one electron with both Al ions, these bonds are weak and their lengths increase by $\sim$10% with dimerization. At the same time the coordination number of the bridging carbons increases to five. This leads to internal steric hindrance of the bridging methyl groups.

The structure has its counterpart in the excitations. High resolution neutron spectroscopy shows two resolved tunnelling transitions [7, 8]. One unresolved line is related to bridging methyl groups where the steric hindrance due to the increased coordination number overcompensates an expected weakening of the rotational potential due to the increased bondlength.

It is expected that with increasing weight/size of the metal ion the dimeric character will be reduced or disappear. $Ga(CH_3)_3$, with a melting point $T_m = -19\,^{\circ}C$, was suggested to possibly represent an intermediate case between dimer and monomer. Crystal structures were determined recently by x-ray crystallography at two temperatures. Just below the melting point a tetragonal space group $P4_2/n$ is found [9]. All $Z = 8$ molecules in the unit cell are equivalent and represent flat triangles. Due to low site symmetry the three methyl groups of a molecule are all different. At the lower temperature $T = 130$ K the symmetry is reduced. A monoclinic space group $C2/c$ ($Z = 16$) is found [10] which is identical to that of $Al(CH_3)_3$. The density calculated from the crystallographic parameters is $\rho = 1.452$ g cm^{-3} and compares well to the value extrapolated from the liquid density $\rho = 1.169$ g cm^{-3} at $T = 273.2$ K and the thermal expansion coefficient $\alpha = 6 \times 10^{-4}$ K^{-1} [11]. Both inequivalent monomers in the unit cell show no symmetry elements connecting their methyl groups. Thus the number of inequivalent methyl groups has doubled to six in the low temperature phase.

The vibrational spectroscopy of $Ga(CH_3)_3$ has been investigated in the gas, liquid and high temperature solid phases by infrared and Raman spectroscopies [12, 13] and most of the internal modes are assigned. The gas phase spectra are consistent with free rotation of the methyl groups. The solid state spectra indicated a reduction in symmetry, however. This was most marked by the splitting of the doubly degenerate antisymmetric GaC_3 stretch mode at 70.3 meV. This was ascribed to a site without a C_3 axis [13] which is confirmed by the crystallography [9]. Neutron vibrational spectra shall be taken from the lowest temperature to complete this knowledge for the second solid phase. Comparison with model calculations will allow us to establish the building unit of the molecular crystal also with spectroscopy.

High resolution incoherent inelastic neutron scattering (INS) can establish methyl rotational tunnelling excitations. Their number and intensities measured at He temperature allow the determination of the number of inequivalent methyl groups and their occurrence probabilities. Tunnelling frequencies can be converted into first order rotational potentials of those groups whose tunnel splittings can be resolved [14]. The temperature dependences of the widths of tunnelling transitions and/or vibrational spectroscopy give—among other things—access to the corresponding methyl librational modes. Quasielastic neutron spectra can supply the activation energies of the rotational potentials of the various methyl rotors. By applying neutron spectroscopy in the full range of molecular eigenenergies (μeV to eV) a fairly complete overview of the dynamics is obtained. Self-consistency has to guide the assignment of modes to lead to unique intermolecular potentials in complex systems.

2. Experiment and results

2.1. Sample preparation

The protonated material was bought at Heraeus, Hanau, Germany. For use in semiconductor technology the material must be extremely pure and can thus be used without further treatment. Part of the liquid material was distilled in a vacuum line from its stainless steel bottle into a glass flask from where it was finally transferred in a glove box under argon atmosphere into a non-reactive stainless steel sample cell of 0.5 mm thickness and lateral dimensions 35×40 mm^2.

2.2. Neutron scattering

2.2.1. Rotational tunnelling. The flat sample was mounted at an angle of +45° to the incoming neutron beam. The high proton density leads to a scattering probability of 27%.

The backscattering spectrometer IN10 at the ILL [15] was used with its Si/Ge offset monochromator. In this setup an energy regime $-32 < \hbar\omega\,(\mu\text{eV}) < 3$ was accessible with an energy resolution of $\delta E \sim 1.5$ μeV. Spectra were taken at various temperatures in the range $1.8 < T\ (\text{K}) < 27.0$. The resolution functions and detector efficiencies were determined by a vanadium run. The background was determined by an empty can run. A selection of spectra is shown in figure 1. Four tunnelling bands with intensity ratios of about 1:1:1:3 are resolved at the lowest sample temperature.

The scattering function of a single tunnelling methyl group labelled i is [16][5]

$$S_i(Q,\omega) = (\tfrac{5}{3} + \tfrac{4}{3}j_0(Qd))\delta(\omega) + (\tfrac{2}{3} - \tfrac{2}{3}j_0(Qd))\{\delta(\omega+\omega_{t_i}) + (\delta(\omega-\omega_{t_i})\}. \tag{1}$$

Here ω_{t_i} means the tunnel frequency. The structure factors contain the spherical Bessel function $j_0(Qd)$ with the proton–proton distance $d = 1.76$ Å. The single-particle model yields the scattering function of N inequivalent methyl groups as a sum of independent rotors

$$S(Q,\omega) = \sum_{i=1}^{N} p_i S_i(Q,\omega) \tag{2}$$

where the occurrence probabilities p_i of species i sum up to unity. From this scattering function one derives the ratios of the inelastic intensity of an individual methyl group to the total elastic intensity $R_{i,el}$ and the ratio $R_{i,j}$ of two different tunnelling transitions

$$\begin{aligned} R_{i,el} &= \frac{I_{inel}}{I_{el}} = p_i\frac{2-2j_0}{5+4j_0} \\ R_{i,j} &= \frac{p_i}{p_j}. \end{aligned} \tag{3}$$

These expressions are valid for a multiline spectrum if all tunnelling transitions are resolved which is the case in our material. The scattering is dominated by the large incoherent scattering cross section of the hydrogen atoms. If we label the tunnelling lines beginning at the highest energy we have $R_{2,1} = R_{3,1} = 1$ and $R_{4,1} = 3$. Based on the crystal structure we describe the spectrum as a superposition of six tunnelling scattering functions of equal weight, however. The description is indeed improved when the most intense line around 5 μeV is represented by three weakly displaced resolution functions. Due to the possibility of coherent elastic scattering the elastic intensity was fitted independently. The theoretical spectrum was convoluted with the measured resolution function (vanadium run). The two outermost tunnelling lines showed an inherent linewidth of 0.27 μeV; the other lines were described by resolution functions. We

[5] Erratum: please note that in the corresponding equation (1) of [8] the parentheses enclosing the tunnelling terms are missing.

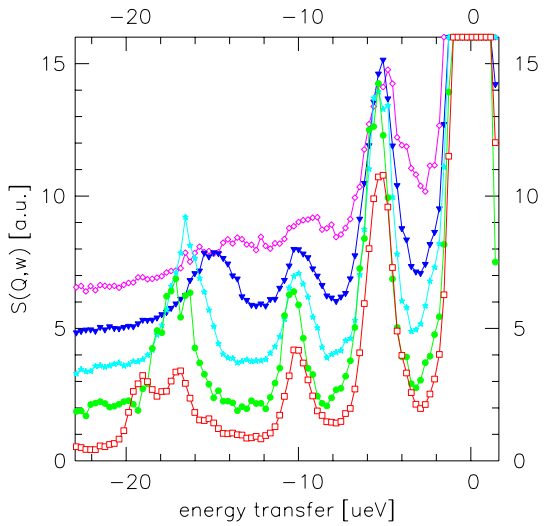

Figure 1. Tunnelling spectra of $Ga(CH_3)_3$ at temperatures 2.0 K (□), 18 K (●), 20.0 K (⋆), 23.5 K (▼) and 25.0 K (◇). Instrument: IN10, ILL, Grenoble, France. Average momentum transfer $Q = 1.64$ Å^{-1}.

can extract the ratio of the integrated inelastic to the elastic intensity as $\sum_i R_{i,el} = 0.23$ for a momentum transfer of 1.6 Å^{-1}. This ratio is independent of occurrence probabilities—which sum up to one—and represents the ratio of inelastic to elastic incoherent structure factors (EISFs) of a single methyl group. Transition energies are shown in the first line of table 1.

With increasing temperature the tunnel lines shift and broaden according to Arrhenius functions [17]

$$\begin{aligned} \Delta\hbar\omega_t &\sim \exp\left(-\frac{E_S}{kT}\right) \\ \Gamma_t &= \Gamma_0 \exp\left(-\frac{E_\Gamma}{kT}\right). \end{aligned} \tag{4}$$

The activation energy of line broadening is $E_\Gamma = E_{01}$ with E_{01} the librational energy of the respective rotor. The same theory delivers E_{01} as an upper limit of the activation energy characterizing the shift of tunnelling lines: $E_S \leqslant E_{01}$. An expansion of the rotor–phonon interaction to higher order [18, 19] introduces a further term, which at low temperature may change the sign of the shift and lead to an unusual increase of the tunnel splitting with increasing temperature. Therefore the meaning of the activation energy of the line shift often becomes unclear.

At a temperature $T = 27.0$ K only the strongest peak at about 5 μeV is still visible. The other lines have transformed into a quasielastic like intensity. In the narrow temperature regime $1.8 \leqslant T(\mathrm{K}) \leqslant 27.0$ and with strongly overlapping lines it is impossible to extract convincing broadenings of each individual transition. The fit has to be stabilized by reasonable restrictions. The low temperature intensities were fixed for all temperatures. While the shift can be well determined the broadening is more difficult to extract in a multi-line spectrum. Unfortunately it is the width to which the theory attributes clear meaning.

Table 1 shows the extracted width and shifts of the tunnel transitions for all temperatures. Figure 2 reproduces these data as Arrhenius plots. The activation energies E_S derived are also shown in table 1. A broadening is most clearly established for the strongest tunnelling line. A straightforward interpretation is misleading, however. Based on the crystal structure, this

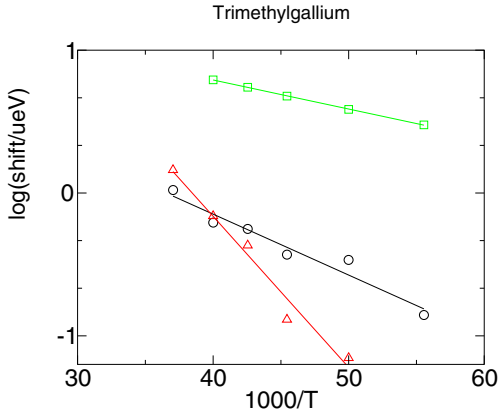

Figure 2. Arrhenius plot of the shift of the tunnelling lines in $Ga(CH_3)_3$. ○, $\hbar\omega_t = 5$ μeV; △, $\hbar\omega_t = 10$ μeV; □, $\hbar\omega_t = 19$ μ eV.

Table 1. Temperature dependence of tunnelling frequencies $\hbar\omega_t$. Two linewidths Γ_t were used, one for the transition at about 5 μeV, and another one for all the other lines. To the two outermost lines an additional width of 0.27 μeV was added. From Arrhenius laws for shift and broadening activation energies $E_{\Gamma,S}$ are derived. The activation energies E_a are assigned according to the comprehensive analysis (see discussion).

Temperature (K)	$\hbar\omega_t$ (μeV)						$\bar{\Gamma}_t$ (μeV)
2	4.98	5.50	5.78	10.06	17.02	19.05	0.01
18		5.49		10.26	16.09	17.22	0.24
20		5.39		10.10	16.15	15.71	0.80
22		5.26		10.04	15.78	14.34	0.55
23.5		5.06		9.75	15.58	13.65	0.91
25		5.01		9.49	15.57	12.96	0.88
27		4.58		8.72	13.62	10.12	1.63
E_S		98		244	—	47	
E_a	310		240		170		

line must be interpreted as a superposition of three lines of equal intensities. Different shifts with temperature of each subline create an apparent line broadening. In our case the apparent broadening transforms into a fine structure of the tunnelling band at the highest temperature investigated since the sublines seem to remain rather narrow but split due to their different and strong shift. This deteriorates also the information contained in the shift of a single tunnelling line: the individual shifts are mixed up into an average one. Again the meaning of corresponding activation energies is questionable.

Some further unusual phenomena are observed (figure 2). The shift of the transition at 10 μeV with temperature is very small and related to a large activation energy. The prefactor of the corresponding Arrhenius function is two orders of magnitude larger than usual and than that of the two other lines. This may indicate that the temperature dependence does not follow a simple Arrhenius function. As in a few other cases the coupling to phonons by shaking and breathing terms [18, 19] may be of similar importance. The respective line shifts can partly compensate each other. This leads to an average activation energy with no physical meaning. We do not consider this value further.

The 19 μeV line shows an anomalously strong shift. This leads to a crossing of the neighbouring lower tunnelling line at about 20 K (figure 1, $\star$). The corresponding Arrhenius description yields a very low activation energy. Interpreted as a librational mode either it would indicate a very unusual potential shape or alternatively an unusually strong coupling to low energy phonons can be assumed. The final analysis will favour the second view.

Thus, the temperature dependence of tunnelling transitions does not yield methyl librational energies and thus cannot contribute to a refinement of the potential shapes in the present case.

2.2.2. Classical reorientational motion. With increasing temperature methyl groups start to reorient classically by jumps over the rotational barrier. This process leads to quasielastic scattering. For a single methyl group rotating in a threefold potential the scattering function is composed of a δ-function and a Lorentzian $L(\Gamma, \omega)$. Inequivalency leads to a superposition of Lorentzians[6]

$$S(Q,\omega) = (1 + 2j_0(Qd))\delta(\omega) + \sum_{i=1}^{N} p_i(2 - 2j_0(Qd))L(\Gamma_i, \omega) \qquad \sum p_i = 1. \tag{5}$$

The Q-dependence of the elastic intensity is characteristic of the jump geometry and is called the EISF. The linewidth Γ_i of the Lorentzian is determined by the average time τ_i between two jumps, $\Gamma_i = \frac{3}{2\tau_i}$, which follows an Arrhenius law

$$\tau_i = \tau_0 \exp\left(-\frac{E_a(i)}{kT}\right). \tag{6}$$

If one can decompose the quasielastic scattering into its n components, a measurement of the temperature dependent linewidths yields the activation energies. Each $E_a(i)$ is generally assumed to represent the distance between the librational ground state and the top of the rotational potential of the ith rotor. To reproduce the observed spectra the outlined scattering function is convoluted with the measured resolution function.

Quasielastic neutron spectra were measured on the cold multichopper time-of-flight spectrometer NEAT [20] at the HMI, Berlin, in the temperature regime $32 < T(\mathrm{K}) < 140$. At an incoming wavelength $\lambda = 7$ Å an energy resolution of $\delta E = 50$ μeV is obtained. An empty can was subtracted from the sample spectra. The six Lorentzians to be fitted into the quasielastic intensity and their relative weights are known from diffraction and tunnelling spectra. Since the different lines are expected to enter the energy window of the spectrometer successively with increasing temperature it could be hoped to extract all the different barrier heights. However, the similarity of some barrier heights made it difficult to disentangle all the individual contributions. The fit often found one-third of the intensity in a broad component and one-half in a narrower component. Thus, restrictions were imposed on the parameters, which otherwise became too strongly correlated. Guided by the answers from the unrestricted fits the finally used scattering function contains three Lorentzians of relative weights 2:3:1. Furthermore the ratio of total inelastic to elastic intensity was fixed. It is most clearly determined at high temperatures and kept constant for the lower ones. Thus, the fit had four free parameters, three linewidths and one intensity factor. Figure 3 shows the final description. At all temperatures $42 \leqslant T(\mathrm{K}) \leqslant 140$ the fits (solid curves) reproduce the measured spectra (symbols) very well. The differences between theory and experiment are easily understood. At negative energy transfers the phonon density of states begins to

[6] Erratum: please note that in [8] the corresponding equation (3) contains the EISF with a wrong sign.

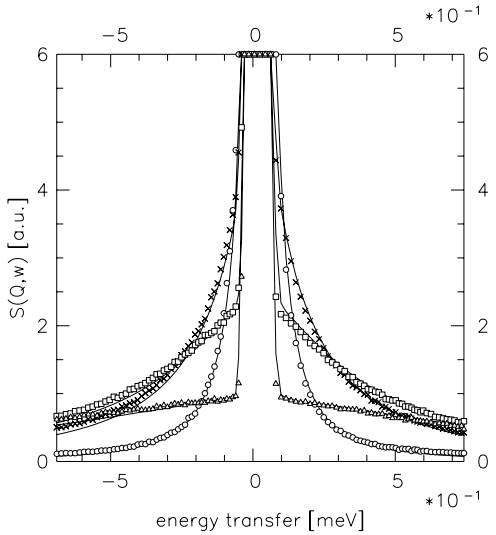

Figure 3. Fits of some quasielastic spectra with three Lorentzians of relative weights 2:3:1. Elastic intensity 60. Sample temperatures are $T = 42.3$ K (○), 71.9 K (×), 91.6 K (□) and 140 K (△). Instrument: NEAT at HMI, Berlin, Germany. $\lambda = 7$ Å.

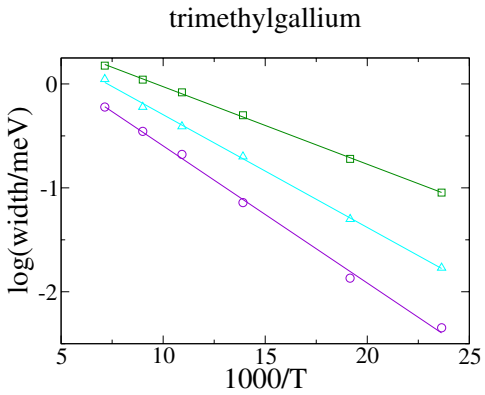

Figure 4. Arrhenius plot of the quasielastic intensity by three Lorentzians. Weight factors: $\frac{1}{3}$ (□), $\frac{1}{2}$ (△), $\frac{1}{6}$ (○).

overlap with quasielastic scattering and the scattering function equation (5) more and more underestimates the measured intensity with increasing temperature. At temperatures below ∼40 K one enters the regime between classical and quantum rotation where the scattering function equation (5) is no longer valid.

With good accuracy the widths of the Lorentzians can be represented by exponential functions with activation energies of 170, 240 and 310 K for the components with relative intensities two, three and one, respectively (figure 4). The prefactors of these Arrhenius laws must be rather similar and are indeed equal within a factor of two. These prefactors are characterisitic of the type of rotor and represent its attempt frequency. With $\Gamma_0 \sim 5$ meV the actual values are similar to those of the many other methyl rotors studied so far.

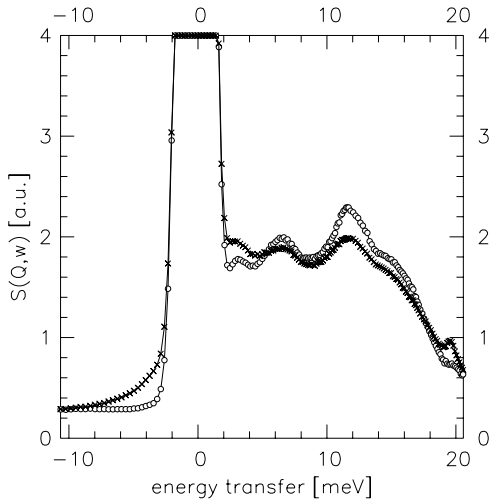

Figure 5. Phonon and librational excitations of $Ga(CH_3)_3$. Instrument: SV29, FZJ, Jülich, Germany. Sample temperature $T = 2.5$ K (O) and $T = 30$ K (×).

2.2.3. Phonon density of states. The thermal time-of-flight spectrometer SV29 at Forschungszentrum Jülich, Germany, was used to determine the excitations of $Ga(CH_3)_3$ in the regime of lattice modes below 25 meV. The elastic energy resolution was 2.0 meV. Figure 5 shows two spectra measured at sample temperatures $T = 2.5$ and 30 K. The low temperature spectrum shows several maxima of the density of states at energies 3.0, 6.4, 11.8, 15.1 and 21 meV. Probably the finite energy resolution hides fine structure or—as often occurs when librational modes coincide with other phonon energies—coupling destroys the Einstein character of a methyl libration and smears out its intensity by dispersion. An additional peak at 27 meV is weakly seen in the third order spectrum with $\lambda = 1.07$ Å. At $T = 30$ K all bands apart from the lowest one are strongly damped which makes them candidates for methyl librational excitations. At $T = 60$ K any inelastic fine structure is lost.

2.2.4. Vibrational modes and ab initio calculations. The INS spectrum was recorded in the wider regime up to 500 meV to detect the methyl torsions and to confirm the earlier optical spectroscopy results. The sample was the same as used for the other neutron spectroscopic measurements and the spectrum was recorded at 14 K using TOSCA [21] at ISIS, Chilton, UK. The spectrum (figure 6(c)) is available from the INS database [22] at www.isis.rl.ac.uk/insdatabase.

The observed intensity of an INS band is given by [23]

$$S(Q, n\omega_i) \propto \sigma \frac{(Q^2\langle u_i^2\rangle)^n}{n!} \exp(-Q^2\langle u_{tot}^2\rangle) \tag{7}$$

where ω_i is the ith mode at frequency ω_i, $n = 1$ for a fundamental, $n = 2$ for a first overtone or a combination line, $n = 3$ for a second overtone or ternary combinations etc. Q is the momentum transfer; $\langle u_i^2\rangle$ is the mean square displacement of the atoms in the mode. $\langle u_{tot}^2\rangle$ is the total mean square displacement of all the atoms in all the modes, both internal and external. σ is the inelastic scattering cross section of the atom. The inelastic scattering cross section of hydrogen is more than an order of magnitude larger than that of C or Ga and since the intensity is dependent on the amplitude of vibration, which is larger for light atoms, the spectra will be dominated

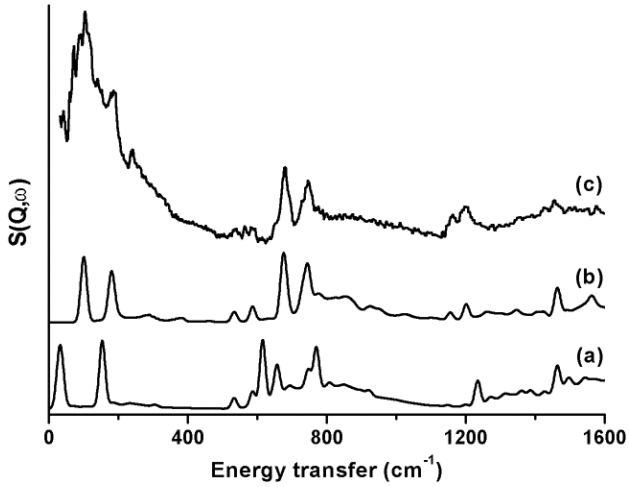

Figure 6. Vibrational spectrum of $Ga(CH_3)_3$. Instrument: TOSCA, RAL, Chilton, UK. Sample temperature $T = 14$ K. (a) *Ab initio* derived INS spectrum of $Ga(CH3)_3$, (b) after adjustment of frequencies to observed values and (c) experimental INS spectrum. 8.07 $cm^{-1} \triangleq 1$ meV.

by motions that involve displacement of hydrogen. The exponential term in equation (7) is a Debye–Waller factor. Equation (7) is based on an isolated molecule approximation, thus dispersion is not included. The narrow linewidths of the modes above 25 meV demonstrate that this is a reasonable assumption for the internal modes in the present case.

The vibrational modes of small molecules can be calculated on a PC using *ab initio* methods. In the present case, density functional theory (DFT) as implemented in the GAUSSIAN98 [24] package was used with the B3LYP functional and 6–31G and 6–31 + G(d, p) basis sets. For the initial structure, a planar GaC_3 skeleton was used. However, the overall symmetry of the molecule depends on the orientation of the C–H bonds and whether they are all equivalent. Several different orientations were considered but all gave similar results for the frequencies, apart from the torsional modes. Most gave negative frequencies for at least one of the torsions. Since GAUSSIAN98 is an isolated molecule calculation, this is consistent with free rotation in the gas phase. Unusually, there was a marked difference between the frequencies calculated using 6–31G and 6–31 + G(d, p) basis sets, with the latter providing the best results.

The output of GAUSSIAN98 includes the atomic displacements for each mode, which can be used to visualize the mode and also to generate the INS spectrum. The program a-CLIMAX [25] was used for this purpose. Figure 6(a) shows the INS spectrum calculated from the GAUSSIAN98 output. The lowest energy modes at 4 meV are the torsions (one of the frequencies is imaginary) consistent with free rotation. The experimental result, figure 6(c), is dominated by the methyl torsions, but these are centred at 12 meV as seen most clearly in figure 5. The band is structured, showing that the methyl torsions are coupled among each other and to phonons by the low site symmetry of the molecule. This also accounts for the different intensities of the calculated and observed bands: for these modes the isolated molecule approximation is not valid. The vibrations at 23 meV are the in-plane and out-of-plane skeletal bending modes. These are correctly calculated for the gas phase molecule at 19 meV. In the solid state they are shifted up by 4 meV. At higher energies, the pattern of intensities is correct although the frequency agreement is poorer. As an empirical correction for the solid state effects, analogous to the scaling factors that are routinely used [26] the individual

Table 2. Vibrational energies measured with the spectrometers SV29 at FZJ and TOSCA at RAL are compared with first principles calculations using the GAUSSIAN program.

Eigenenergies (meV)		
INS	GAUSSIAN94	Mode character
3.0		Acoustic phonons
6.4		Acoustic phonons
11.8		Torsion CH_3
15.1		Torsion CH_3
21	20	Out-of-plane skeletal bending
23		In-plane skeletal bending
27		Excited torsion?
65	68	Antisymm. skeletal stretch
71		Bending around Ga–C bonds
83		
94	96	Out-of-plane whole mol.
146	155	Symm. deformation CH_3 (umbrella)
	180	Symm. bend CH_3
	363, 374, 378	CH_3 stretch

bands are moved to the observed positions without altering their intensity. Figure 6(b) shows the spectrum after moving the individual bands, without altering their intensity, to the observed positions. In essence, this amounts to scaling the diagonal force constants and assuming that the off-diagonal ones are unchanged. In the case of the methyl torsions, because they are so strongly altered by the crystal lattice, their intensity is reduced by two-thirds. If this is not done the Debye–Waller factor of equation (7) is so large that no modes above 25 meV are visible. With these changes and inclusion of combination lines involving up to two quanta the result shown in figure 6(b) is obtained. The agreement between observed and calculated is excellent, confirming the assignments given in table 2.

The splitting in the antisymmetric GaC_3 stretch mode at 70.3 meV is clearly seen in the spectrum but is not reproduced by the calculations. Considering just the GaC_3 skeleton and using a simple valence force field showed that to generate a 1.2 meV splitting a 5% difference in force constants for two of the Ga–C bonds was necessary. Assuming that the force constant and bond distance are inversely related, such a difference is much larger than the variation in the Ga–C distances observed crystallographically [9]. This indicates that the stretch is coupled to the rocking and bending modes as suggested previously [13].

All observed characteristic energies are shown in table 2.

3. Discussion

3.1. Structural information from spectroscopic data

The internal modes can be used to identify spectroscopically the building unit of the molecular crystal by an eigenmode analysis. Flat triangular monomers are found in agreement with the minimum energy configuration obtained in a quantum chemical calculation using the GAUSSIAN program [24]. Many of the calculated characteristic internal modes are seen in the vibrational neutron spectrum. The assignment is given in table 2. The modes at 21, 65, 71 and 94 meV are only present for isolated monomers. A run of GAUSSIAN based on a dimeric unit did not contain transitions at these energies.

High resolution spectra on the other hand are sensitive to the symmetry within and between molecules as established in the space group of the crystal. As long as there is no contamination of the elastic line the ratio of the total inelastic/tunnelling and the elastic intensities allows us a check of whether all tunnelling transitions are observed. IN10 has no bank of diffraction detectors like IN16 to check the presence of Bragg intensity. Therefore this test was made at low momentum transfer where the probability of being perturbed by a diffraction line is very small. For a scattering angle $2\theta = 62°$ which corresponds to a momentum transfer $Q = 1.01$ Å^{-1} the experimentally determined value $R_{exp} = \frac{I_{inel}}{I_{el}} = 0.14$ fits rather well with the expected ratio $R_{th} = 0.13$. The low value $R_{exp} = 0.23$ found for $Q = 1.6$ Å in section 2.2.1 reveals the presence of Bragg intensity at larger scattering angles. Thus the transitions of all methyl groups are inside the window of the spectrometer. The six observed transitions are most easily explained by two inequivalent monomers of no internal symmetry in the unit cell which is indeed the result of the crystal structure determination [10].

3.2. Rotational potentials

Rotational potentials are expressed in form of Fourier series

$$V(\varphi) = \sum_{n=1}^{N} \frac{V_{3n}}{2}(1 - \cos(3n\varphi - \varphi_{3n})). \tag{8}$$

The potential determines the measured excitations by eigenvalues of the single-particle Schrödinger equation [16]

$$\left(-B\frac{\partial^2}{\partial\varphi^2} + V(\varphi)\right)\Psi_i = E_i\Psi_i. \tag{9}$$

Tunnel splittings are uniquely well defined but without further knowledge they allow the extraction of the simplest approximation to the real rotational potential only, the term V_3.

With increasing number of observed excitations of the hindered rotor higher order Fourier components of the potential can be determined. In this procedure φ_{3n} is set to 0° or 180°, which equivalently can be expressed by a positive or a negative sign of the corresponding V_{3n}. This latter convention is used in the following. Based on the temperature dependence of tunnelling lines one often can make assignments of E_{01} to the respective methyl groups. In principle it would be possible to derive barrier heights V_{3i} up to second order, $N = 2$, and calculate corresponding activation energies E_a (table 3). In our case overlapping tunnelling lines do not allow this procedure, unfortunately. Therefore tunnelling transitions are arbitrarily combined with bands of the phonon density of states. The interpretation as librational modes is again only a likely hypothesis. Some combinations are found to be impossible in the single-particle model and are immediately excluded. For example a small tunnel splitting is inconsistent with a low lying librational mode. For the remaining solutions the activation energies measured by quasielastic scattering are introduced as a control parameter. Only combinations of eigenmodes which yield at the same time measured barrier heights and the required occurrence probabilities are accepted. The last column of table 3 shows the final assignment which involves a consistent description of all spectroscopic results.

Guided by the slow activation energy of the shift of the tunnel transition the mode at 19 μeV could be combined with a very low librational mode leading to the highest activation energy in a strongly deformed rotational potential. Alternatively a close to threefold potential with a medium energy libration and a low activation energy is possible. This potential is more likely because the systematics is in favour of close to threefold potentials [27]. The choice of this potential involves the small activation energy of the shift of the tunnel band at 19 μeV

Table 3. Rotational potentials derived from tunnel frequencies $\hbar\omega_t$ and the first librational level E_{01} extracted from the strongest peaks of the DOS. Combination with the measured activation energies E_a^{exp} allows consistent assignment. The almost degenerate tunnelling mode around 5 μeV is found to contain different rotor systems.

$\hbar\omega_t$ (μeV)	Rel. int.	E_{01} from DOS	V_3 (meV)	V_6 (meV)	E_a^{calc} (K)	E_a^{exp} (K)	Rel. int.	Assignment
4.5–6	$\frac{1}{2}$	11.8	34.1	2.5	302	310	$\frac{1}{6}$	$\frac{1}{6}$
4.5–6		15.0	29.0	9.7	235	240	$\frac{1}{2}$	$2 \times \frac{1}{6}$
10.06	$\frac{1}{6}$	11.5	30.4	−0.6	238	240		$\frac{1}{6}$
17.02	$\frac{1}{6}$	12.0	22.0	6.2	168	170	$\frac{1}{3}$	$\frac{1}{6}$
19.05	$\frac{1}{6}$	11.6	22.0	5.5	170	170		$\frac{1}{6}$
19.05	$\frac{1}{6}$	6.0	39.3	−26.2	352	310		—

with temperature being assigned to strong coupling to low energy phonons by a breathing term [18, 19]. The assignment is further supported by the fact that the large activation energy is needed to get a potential for the smallest tunnel splitting. As a consequence of this next assignment the tunnel transition at 5 μeV is another time confirmed to be a multiplet because the largest activation energy has only a multiplicity of $\frac{1}{6}$. This means that one component of this almost degenerate tunnelling band feels a clearly distinct rotational potential. The remaining assignments are then straightforward and consistent with the experience that larger tunnel splittings are connected with lower barriers.

4. Conclusion

Trimethyl gallium is a member of the group IIIA alkyls. In contrast to trimethyl aluminium the building unit is the monomer. This diffraction result is fully supported by the mode analysis of internal vibrational excitations. Similarly, rotational tunnelling and quasielastic spectroscopy show that all rotational potentials are of comparable magnitude and thus do not reflect any unusual bonding as in the case of trimethyl aluminium [8].

The complexity of the present material with its large number of six inequivalent rotors requires a comprehensive spectroscopic investigation. Rotational tunnelling allows the identification of the number of inequivalent methyl groups. Due to rather similar rotational potentials quasielastic scattering cannot resolve all these different rotors. The density of states on the other hand is difficult to interpret. The identification of librational modes and their assignments to tunnelling transitions require the analysis of damping of tunnelling modes with temperature [1, 17]. In the present case overlapping lines affect the broadening of tunnelling transitions with large errors, however. On the other hand the more easily observable lineshift is of little use since coupling to phonons may cause shifts into opposite direction with an unpredictable net effect—at least at small shifts. Due to the lack of this safe possibility to combine tunnelling and librational excitations, all possible combinations of tunnelling transitions with librational density of states were examined. The selection of the right combinations takes quasielastic spectra into account: only combinations which yield the observed barrier heights together with their occurrence probabilities can be reliable. The resulting interpretation shows that the strong tunnelling band around 5 μeV is indeed a multiplet and that the strong shift of the tunnelling line at 19 μeV with temperature is not related to a low energy librational mode but must be attributed to strong coupling to phonons.

The main conclusion is that only a combination of all spectroscopic information allowed us to achieve a consistent understanding of the complex molecular crystal $Ga(CH_3)_3$.

Acknowledgment

We thank Dr Hardtdegen of ISG1 of Forschungszentrum Jülich for supplying the sample material for the outlined experiments.

References

[1] Müller-Warmuth W, Duprée K H and Prager M 1983 *Z. Naturf.* a **39** 66
[2] Prager M and Langel W 1986 *J. Chem. Phys.* **85** 5279
[3] McGrady G S, Turner J F C, Ibberson R M and Prager M 2000 *Organometallics* **19** 4398
[4] Vranka R G and Amma E L 1967 *J. Am. Chem. Soc.* **89** 3121
[5] Lewis P H and Rundle R E 1953 *J. Chem. Phys.* **21** 986
[6] Huffman J C and Streib W E 1971 *Chem. Commun.* **1971** 911
[7] Prager M, Grimm H, Parker S F and McGrady J 2000 *Physica* B **276–278** 250
[8] Prager M, Grimm H, Parker S F, Lechner R, Desmedt A, McGrady J and Koglin E 2002 *J. Phys.: Condens. Matter* **14** 1833
[9] Mitzel N, Lustig C, Berger R and Runeberg N 2002 *Angew. Chem. Int. Ed.* **41** 2519
[10] Boese R, Bläser W and Prager M unpublished
[11] *Gmelin Handbook* Ga-Org. Comp. 1 p 27
[12] Durig J R and Chatterjee K K 1981 *J. Raman Spectrosc.* **11** 168
[13] McKean D C, McQuillan G P, Duncan J L, Sheppard N, Munro B, Fawcett V and Edwards H G M 1987 *Spectrosc. Acta* **43A** 1405
[14] Prager M and Heidemann A 1997 *Chem. Rev.* **97** 2933
[15] www.ill.fr/YellowBook/
[16] Press W 1981 *Single Particle Rotations in Molecular Crystals (Springer Tracts in Modern Physics vol 81)* (Berlin: Springer)
[17] Hewson A C 1982 *J. Phys. C: Solid State Phys.* **15** 3841–55
[18] Häusler W 1990 *Internal Report* PTB-PG-3 Physikalisch Technische Bundesanstalt
[19] Würger A 1989 *J. Phys.: Condens. Matter* **1** 6901
Würger A 1989 *Z. Phys.* B **76** 65
[20] Lechner R E, Melzer R and Fitter J 1996 *Physica* B **226** 86
[21] Colognesi D, Celli M, Cilloco F, Newport R J, Parker S F, Rossi-Albertini V, Sacchetti F, Tomkinson J and Zoppi M 2002 at press
[22] Parker S F and Champion D J 1999 *Int. J. Vib. Spectrosc.* **3**
http://www.ijvs.com/volume3/edition3/section1.htm#Ed
[23] Tomkinson J 1994 *Neutron Scattering from Hydrogen in Materials* ed A Furrer (Singapore: World Scientific) p 168
[24] Frisch M J, Trucks G W, Schlegel H B, Scuseria G E, Robb M A, Cheeseman J R, Zakrzewski V G, Montgomery J A Jr, Stratmann R E, Burant J C, Dapprich S, Millam J M, Daniels A D, Kudin K N, Strain M C, Farkas O, Tomasi J, Barone V, Cossi M, Cammi R, Mennucci B, Pomelli C, Adamo C, Clifford S, Ochterski J, Petersson G A, Ayala P Y, Cui Q, Morokuma K, Malick D K, Rabuck A D, Raghavachari K, Foresman J B, Cioslowski J, Ortiz J V, Baboul A G, Stefanov B B, Liu G, Liashenko A, Piskorz P, Komaromi I, Gomperts R, Martin R L, Fox D J, Keith T, Al-Laham M A, Peng C Y, Nanayakkara A, Gonzalez C, Challacombe M, Gill P M W, Johnson B, Chen W, Wong M W, Andres J L, Gonzalez C, Head-Gordon M, Replogle E S and Pople J A 1998 *Gaussian 98* Revision A.7 (Pittsburgh, PA: Gaussian)
[25] Champion D J, Tomkinson J and Kearley G J 2002 *Appl. Phys.* A at press
[26] Ramirez-Cuesta A J and Tomkinson J 2002 *Neutron News* at press
[27] Clough S, Heidemann A, Horsewill A, Lewis J D and Paley M N J 1982 *J. Phys. C: Solid State Phys.* **15** 2495